# We are IntechOpen,
# the world's leading publisher of
# Open Access books
# Built by scientists, for scientists

## 6,900
Open access books available

## 185,000
International authors and editors

## 200M
Downloads

## 154
Countries delivered to

Our authors are among the

## TOP 1%
most cited scientists

## 12.2%
Contributors from top 500 universities

**CLARIVATE ANALYTICS**
**BOOK CITATION INDEX**
**INDEXED**

**WEB OF SCIENCE**™

Selection of our books indexed in the Book Citation Index
in Web of Science™ Core Collection (BKCI)

## Interested in publishing with us?
## Contact book.department@intechopen.com

# Evaluating Cooling Tower Scheme and Mechanical Drag Coefficient Formulation in High-Resolution Regional Model

Miao Yu and Shiguang Miao

Additional information is available at the end of the chapter

## Abstract

A cooling tower scheme considering quantitative sensible and latent heat flux released from air condition was implemented in building energy model (BEM) and coupled to the regional model (WRF). A mechanical drag coefficient formulation was implemented into the WRF/BEM to improve the representation of the wind speed in complex urban environments. Two simulations used default WRF/BEP+BEM and improved WRF/BEM to estimate the improvement effects focusing on dry day and wet day for summer 2015, respectively. The cooling tower system in commercial area not only induces the significant increase of the anthropogenic heat partition by 90% of the total heat flux releasing as latent but also further changes the surface heat flux feature. When the cooling tower is introduced, averaged surface latent heat flux in urban area is increased to about 60 $W\cdot m^{-2}$ with the peak of 150 $W\cdot m^{-2}$ in dry day and 40 $W\cdot m^{-2}$ with the peak of 150 $W\cdot m^{-2}$ in wet day. Maximum and minimum temperature error improved by 2–3 degrees. In the vertical model, the performance of boundary layer structure in rural area is much better than in urban area. The average wind speed error improved by 2–3 m/s in urban area with new calculation scheme.

**Keywords:** cooling tower, drag coefficient, regional model, high-resolution

## 1. Introduction

The world's population is coming increasingly urbanized, and most of this additional urbanization occurs in developing countries [1]. The land-use change and the anthropogenic heat release induced by urbanization have been recognized as important factors that have serious impacts on climate at regional scales [2–4]. There is plenty of evidence that the regional climate

effect of urban is significant [5–9]. And urban impacts are becoming more and more important in fine weather forecasting. It is difficult to distinguish the impact of land-use change and artificial heat emissions on regional climate in the observation. But numerical model can be used to solve this problem [10]. Feng et al. [11] employed WRF coupled with single-layer urban canopy model (UCM) to investigate urban land-use change and anthropogenic heat release on regional climate in China and indicated that impact of anthropogenic heat release is larger than urban land-use change.

Anthropogenic heat is one contributor to the urban heat islands which destroyed the near-surface inversion and increased the stratification instability [12]. Anthropogenic heat release is the extra heat flux which can change the surface energy balance [13, 14]. Energy consumption from buildings is an important part of anthropogenic heat release that may modify near-surface energy balance [15].

Sailor [16] provides a historical perspective on the development of models of urban energy consumption and anthropogenic impacts on the urban energy balance. It indicated that there is a positive feedback cycle that higher temperatures result from greater amounts of energy used for air cooling in most urban area [17]. Global modeling results indicated that heat release from building is the largest contributor (89–96%) to the large-scale urban consumption of energy [12]. Future climate experiments by GCMs show anthropogenic heat flux can cause annual-mean warming of 0.4–0.9°C over large industrialized regions although global-mean anthropogenic heat flux is small [18]. The temperature increased by anthropogenic heat not only depends on the amount of heat released but also on orographical factors [19]. The amount of heat released at night is lower than at day, but the temperature increase is nearly three times greater [20]. Global model shows that the extra heat from energy consumption over the 86 major metropolitan can cause up to 1° of warming in winter seasons [21].

Recent regional modeling results show that anthropogenic heat flux from building has a significant impact on temperature simulation on urban area [22]. The heat release of air condition caused about 1–2°C warming in summer commercial area [23]. The study of Pairs also indicated that about 0.5°C results from anthropogenic heat release and points out the air condition makes important contributions to surface warming [24]. A study on three major urban agglomerations of China suggests that contribution of anthropogenic heat release to warming is larger than the land-use change [11].

But the performance of current urban canopy model is not satisfied for artificial heat emissions in urban area [11, 25]. Both UCM and BEM take the anthropogenic heat as extra surface sensible flux and can only recognize the diurnal variation [26]. But UCM and BEM cannot describe the energy exchange between anthropogenic heat flux and the urban boundary layer sensible heat flux which leads to energy balance in the boundary layer destroyed. It is note-worthy that anthropogenic heat release includes not only sensible heat flux but also latent heat flux. Anthropologic latent heat flux from urban area is ignored by UCM and BEM. Building energy model that can accurately describe energy balance mechanism of urban boundary layer and includes anthropogenic heat release urgently needs development.

The development of BEM model has solved the problem to a great extent [27]. Current BEM model is capable of describing (1) the heat diffusion through walls, roofs, and floors, (2) the

natural ventilation and the radiation exchanged between the indoor surfaces, (3) the heat from occupants and equipment, and (4) the energy consumption from air condition.

Although BEM has the ability to simulate the building energy-exchange process as mentioned above, the performance is not satisfied enough especially for the high-resolution forecast in urban area [3, 25, 28]. Air condition releasing is treated as sensible heat flux to potential temperature equation when couples to BEP and regional model [29]. Simulated temperature in urban area is always obviously higher than the observation by current WRF/BEM model. Assessment report in Beijing shows that latent heat flux maximum simulated by WRF/BEM is only 40 $W \cdot m^{-2}$ while the observation is about 230 $W \cdot m^{-2}$ [25]. Errors of simulated heat flux directly lead to underestimate the humidity and further affect the performance of rainfall. In most commercial buildings, anthropogenic heat can be associated to heat release from air conditioning systems. Most air conditioning systems use evaporative cooling that releases a mixture of sensible and latent heat to the environment [30].

Many studies show that the energy consumption of air condition from building is gradually increasing as the frequency of heat wave is increasing [31]. And heat release from the building air condition system is one of the primary sources of anthropologic latent heat flux in urban area [29, 32–35]. Although heat released by air condition is considered in the current WRF/BEM, the performance is still not satisfied. Previous studies have indicated that heat released by air condition in some megacities is equal to or more than half of the surface sensible flux [23]. Simulation results show that contribution of heat released by air condition to summer warming can exceed $1°$ in the megacities [23, 36, 37], and contribution to nighttime temperature can reach $2°$ [29].

However, most air condition systems use evaporative cooling that releases a mixture of sensible and latent heat to the environment. In summer, 50–80% of their heat released by evaporative-cooled systems is in the form of latent heating [38]. In China, metropolitan electricity consumption report shows that most important energy consumption in building comes from air condition system whether in commercial or residential area [39]. Air condition usage report about Chinese metropolitan indicated that the ratio of sensible and latent heat flux by different types of air condition emissions is 20 and 80%, respectively [39].

So how to correctly describe the latent heat flux released by air condition in high-resolution model is an urgent problem to solve. It has shown that a BEM coupled with a cooling tower model can improve the model performance of temperature [30]. Cooling tower scheme will obviously improve model performance of the energy exchange ability between building and its surroundings and urban boundary layer balance.

Beijing power consumption is gradually increasing from 1978 to 2015, and the proportion of electricity consumed by residents is also gradually increasing (Beijing Municipal Bureau of Statistics website). It is noteworthy that heat released from building air condition is the important component of summer electricity consumed by residents. Namely, heat flux released by air condition system in Beijing's urban area becomes one of the primary sources of summer anthropologic heat as other big cities. In order to modify the simulation of heat flux released by air condition, a new cooling tower scheme [30] was coupled to rapid-refresh multi-scale analysis and prediction (RMAPS).

Parameterizations using the specific input parameters describe the complex arrangement of buildings and streets in an urban environment. However, simulations using this type of data reproduce fine-resolution features that are not clearly reproducible by traditional methods [10, 29].

In order to represent the effects of horizontal and vertical building surfaces of momentum, heat, and turbulent kinetic energy (TKE) equations, the building effect parameterization and the building energy model (BEP + BEM) [40] have been introduced. In the relevant equations, new terms about frictional and drag forces on the mean flow and the increase of the TKE between buildings are introduced. This scheme assumes drag coefficient is a constant. That is inaccurate because the magnitude of the drag is decided by building density in highly heterogeneous urban environments. A new formulation has been implemented in the BEP + BEM system to calculate the values of the drag coefficient based on the building plan-area fraction to improve the airflow simulation in the urban boundary layer. The performance of this drag formulation has been evaluated in an idealized urban configuration using computational fluid dynamical (CFD) simulations [27].

Our aims are as follows:

1.  To improve the performance of BEM using the cooling tower scheme and drag formulation.

2.  To evaluate the forecast performance of the improved RMAPS coupled with improved BEM in summer Beijing
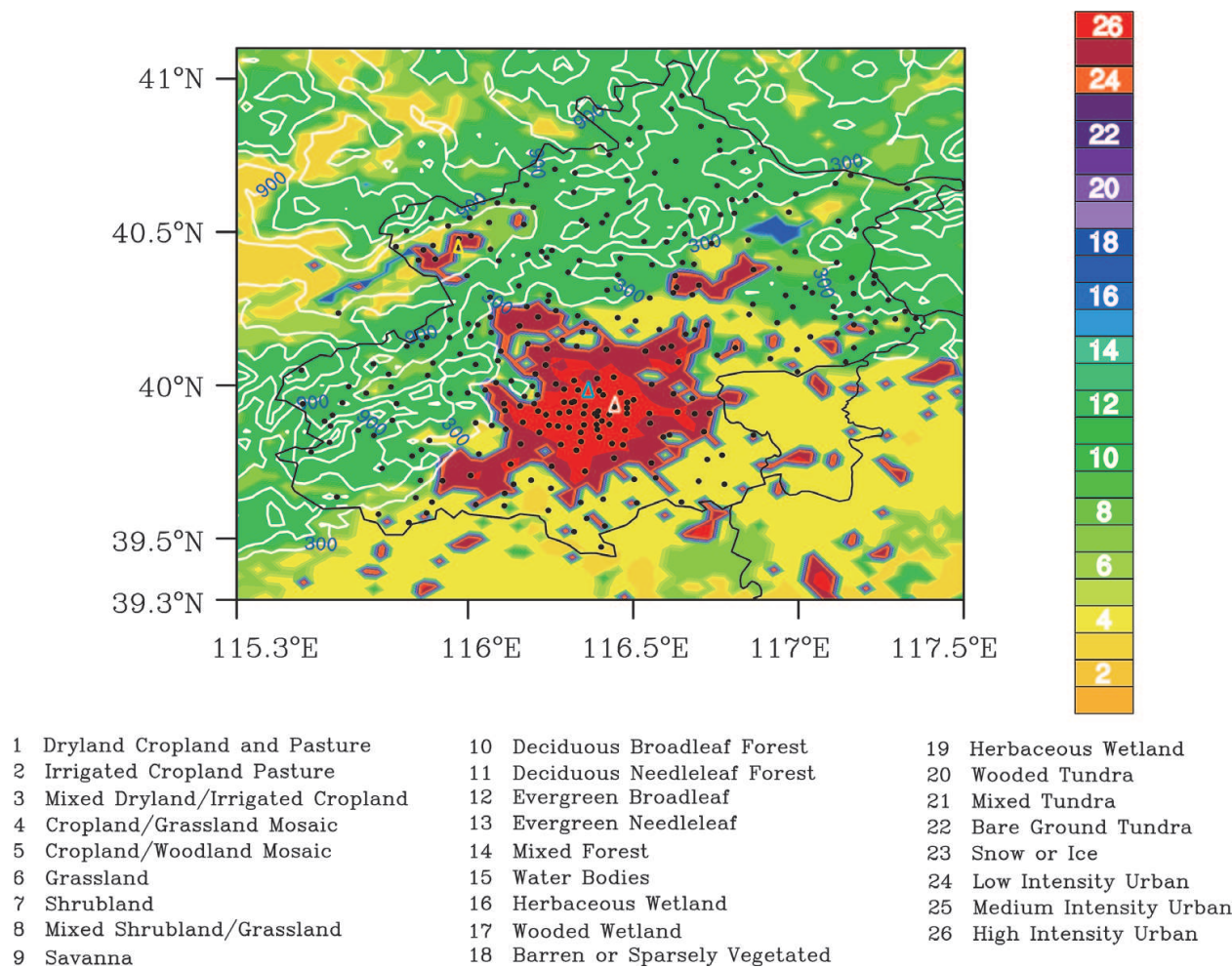
Details of the data and the experimental design are given in Section 2. The performance of improved RMAPS is evaluated in Section 3. We summarize the findings and discuss our results in Section 4.

## 2. Data, model description, and experimental design

The surface temperature and humidity data were obtained from 294 meteorological stations operated by the Beijing Meteorological Bureau (**Figure 1**). Vertical temperature data was gathered from a radiometer located at 39.8°N, 116.46°E. Heat flux data used in this study were obtained from the Beijing meteorological tower (39.97°N, 116.37°E), which is 325 m high and located in North Beijing.

This study used operational rapid-refresh multi-scale analysis and prediction system (RMAPS) based on modified version of the WRF model (ARW versions 3.5.1), and its data assimilation system (WRFDA v3.5) was developed by the Institute of Urban Meteorology, China Meteorological Administration, Beijing [25]. The system starts with ECMWF global forecasts (at 3-h intervals) and terminates with hourly weather forecasts. Initial conditions is adjusted by WRFDA-ingested including S/C band weather radar, ground-based global positioning system meteorology (GPS-MET), radiosonde, Aircraft Meteorological Data Relay (AMDAR), and AWS surface observations. Three domains are designed for the current study with horizontal

1   Dryland Cropland and Pasture
2   Irrigated Cropland Pasture
3   Mixed Dryland/Irrigated Cropland
4   Cropland/Grassland Mosaic
5   Cropland/Woodland Mosaic
6   Grassland
7   Shrubland
8   Mixed Shrubland/Grassland
9   Savanna

10   Deciduous Broadleaf Forest
11   Deciduous Needleleaf Forest
12   Evergreen Broadleaf
13   Evergreen Needleleaf
14   Mixed Forest
15   Water Bodies
16   Herbaceous Wetland
17   Wooded Wetland
18   Barren or Sparsely Vegetated

19   Herbaceous Wetland
20   Wooded Tundra
21   Mixed Tundra
22   Bare Ground Tundra
23   Snow or Ice
24   Low Intensity Urban
25   Medium Intensity Urban
26   High Intensity Urban

**Figure 1.** High-resolution land-use map in model. Black dots show the 294 weather stations. The white triangle shows the location of a 325 m meteorological tower (39.97°N, 116.37°E); the blue triangle shows the location of the Naojiao station (39.8°N, 116.46°E); and the yellow triangle shows the location of the Yanqing station (40.45°N,115.97°E).

grid spacings of 9, 3, and 1 km. The locations of the nested urban domains are shown in **Figure 2**. NDOWN provides boundary conditions for the 1-km Domain-3 model from its 3-km output, and VDRAS output is assimilated into the 1-km domain via FDDA [41]. Land-use map (**Figure 1**) is based on 30-m Landsat data for the year 2010, including three urban land types according to gridded urban-fraction values [42]. Parameterization schemes used in this study are listed in **Table 1**.

In order to improve the current forecast model, a cooling tower scheme was incorporated to the BEP + BEM and was coupled with RMAPS. Beijing is taken as the case study to investigate anthropogenic heat impact of dense urban environment. Although the cooling tower scheme has been used to the regional model in previous work, verification and evaluation for improved model are not sufficient especially in vertical stratification. This work used multiple intense observation data to evaluate the improvement effect of the new cooling tower scheme.
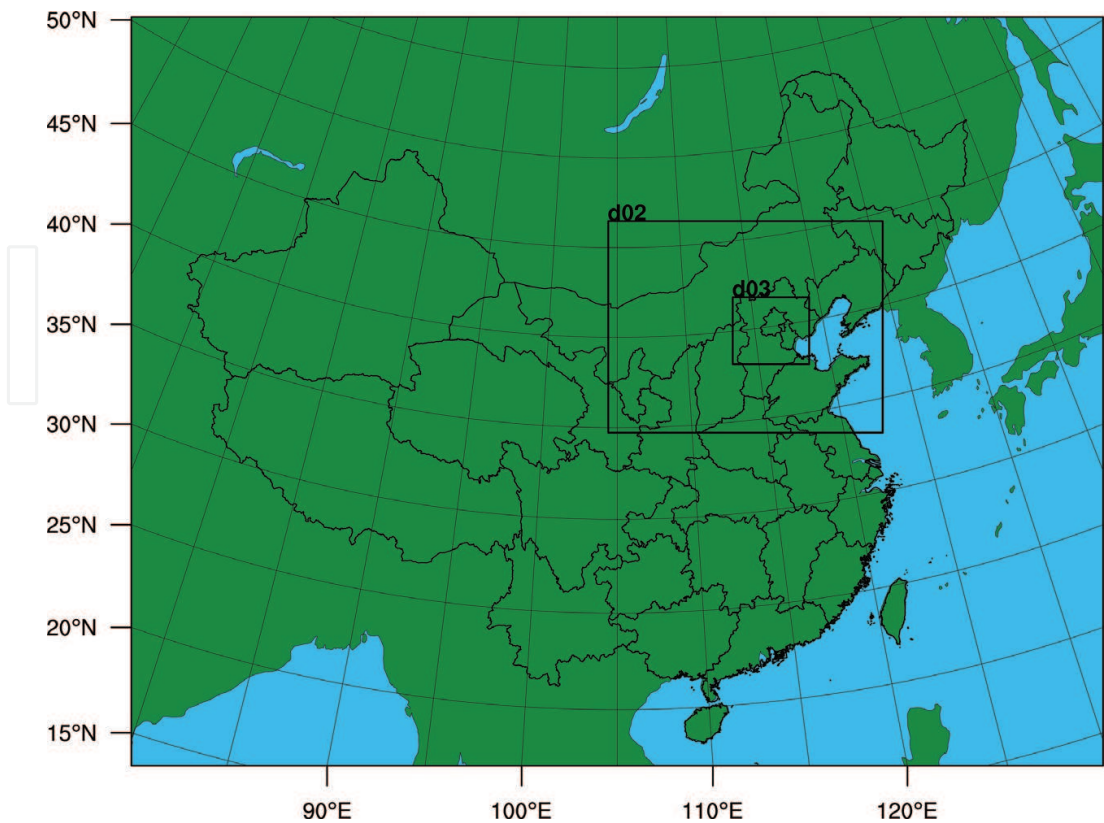
**Figure 2.** Domain configuration and location of the study area.

|  | D1 | D2 | D1 |
|---|---|---|---|
| Models and versions | WRFDA v3.5.1 + WRF v3.5.1 |  | WRF v3.5.1 |
| Horizontal grid points | 649 × 400 | 550 × 424 | 460 × 403 |
| Δx (km) | 9 | 3 | 1 |
| Vertical layers | 50 |  |  |
| Cumulus physics | Kain-Fritsch | None | None |
| LW radiation | RRTM |  |  |
| SW radiation | Dudhia |  |  |
| Microphysics | Thompson |  |  |
| PBL physics | ACM2 | BouLac |  |
| Urban physics | SLUCM | BEP | BEP + BEM |

**Table 1.** Modeling setting and parameterization options.

The computing method is as follows:

Based on the first law of thermodynamics, heat exchange equation between air condition system and the external atmosphere is defined as

$$Q = C_{min}(T_{wo,\,cond} - T_{wi,\,cond}) = C_{min}(T_{Refi} - T_{wi,\,cond}) \tag{1}$$

$$T_{wi,\,cond} = T_{wo,\,CT} = T_{wb,\,air} \tag{2}$$

$$T_{wo,\,cond} = T_{wi,\,CT} \tag{3}$$

where Q is the total heat transfer from the building calculated by BEM, $T_{wi,\,cond}$ is the water temperature entering the air condition system, $T_{wo,\,cond}$ is the water temperature leaving the air condition, $T_{wi,\,CT}$ is the water temperature entering the cooling, $T_{wo,\,CT}$ is the water temperature leaving the cooling tower (CT), and $C_{min}$ is the minimum thermal capacitance between the water and the refrigerant [43]. It is assumed that the cooling tower is able to bring the water entering the air conditioning to its minimum value of the wet bulb temperature. This wet bulb temperature $T_{wb,\,air}$ is calculated from [44–48]:

$$\begin{aligned} T_{wb,\,air} = T_{air}atan\left[0.151977(RH\% + 8.313659)^{1/2}\right] \\ + atan\,(T_{air} + RH\%) - atan(RH\% - 1.676331) \\ + 0.00391838(RH\%)^{3/2}atan(0.023101RH\%) - 4.686035 \end{aligned} \tag{4}$$

where $T_{air}$ is air temperature and $RH$ is relative humidity.

The effectiveness, ε, for the cooling tower is defined as:

$$\varepsilon = \frac{Q}{m_a(h_{sai} - h_{ai})} \tag{5}$$

where $h_{ai}$ is the enthalpy of inlet air and $h_{sai}$ is saturated enthalpy of inlet air.

Finally, the outlet air temperature $T_{ao}$ can be obtained from the following equations using an iterative scheme:

$$Q = m_a(h_{ao} - h_{ai}) \tag{6}$$

$$h_{ao} = h_{ai} + \varepsilon(h_{sai} - h_{ai}) \tag{7}$$

$$C_pT_{ao} + q_{vao}(C_{pw} + L) = h_{ao} \tag{8}$$

$$q_{vao} = 0.62198\frac{e}{P - e} \tag{9}$$

$$e = 6.11 \times 10^{\frac{7.5T_{ao}}{237.7+T_{ao}}} \tag{10}$$

where $q_{vao}$ is absolute humidity or mixing ratio.

Due to the effect of complicated urban surface, the structure of the meteorological field in the urban boundary layer is different from other surfaces. Impervious vertical surfaces of buildings induce a drag force that produces a loss of momentum that changes the flow field in near-surface atmospheric boundary layer. The drag coefficient (Cd) is an important component for

calculating the magnitude of the momentum flux induced by buildings in urban canopy models. According to previous studies over urban environments and wind-tunnel measurements of, Cd is assumed as a constant (0.4) in default WRF/BEM [40]. However, Cd could vary with building packing densities. An analytical relation proposed by Salamanca and Martilli [27] has been implemented into the BEP + BEM system to estimate the drag coefficient as a function of the building plan-area fraction as follows:

$$Cdeq\,(\lambda p) = \begin{cases} 3.32 x\,\lambda p^{0.47} & for \;\; \lambda p \leq 0.29 \\ 1.85 & for \;\; \lambda p > 0.29 \end{cases} \tag{11}$$

This formulation represents an improvement compared to using a constant drag coefficient, and it is necessary to assess this for a real complex urban underlay.

We evaluated the whole summer (from June 1 to September 30) simulation to evaluate the performance of the RMAPS coupled to the cooling tower model and drag scheme (AC + VD). The forecast results by default RMAPS were used as control run (CTL).

## 3. Results

### 3.1. Effect on diurnal pattern

The significant difference between CTL and AC + VD is in latent heat released from the building because AC + VD improved the heat flux released from the building to the environment. Maximum sensible heat flux from air condition in CTL is about 180 W·m$^{-2}$, while it is reduced to 20 W·m$^{-2}$ in AC + VD (**Figure 3a** and **b**). Meanwhile latent heat flux from air condition is increased by AC + VD during daytime. Thermal exchange between building and
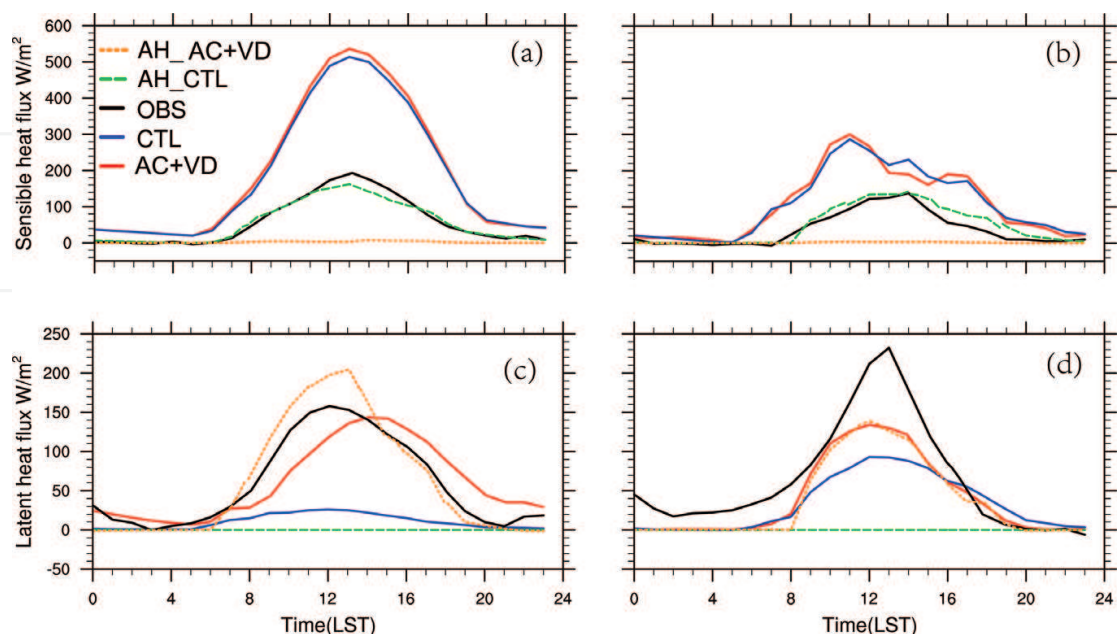


**Figure 3.** Averaged diurnal pattern of heat flux (W·m$^{-2}$). (a) Sensible heat flux in dry day; (b) sensible heat flux in wet day; (c) latent heat flux in dry day; and (d) latent heat flux in wet day.

its external atmosphere simulation is an inadequate capability in CTL. AC + VD not only increase the latent heat flux released from building but also improve simulation ability of heat exchange.

We evaluate sensible and latent heat flux in the dry day first. Based on the heat flux observation by Beijing tower in 140 m, sensible heat flux is less than 20 W·m$^{-2}$ in the nighttime, while CTL overestimate sensible heat flux about 50 W·m$^{-2}$ in the nighttime (**Figure 3a**). It has largely solved this problem by AC + VD during the dry days. But in the wet days, sensible heat flux is still overestimated in nighttime simulated by both CTL and AC + VD. In the daytime, observed sensible heat flux reaches the maximum (200 W·m$^{-2}$) at 1400 LST; both CTL and AC + VD overestimate the sensible heat flux in urban area (**Figure 3a** and **b**). Sensible heat flux simulated by CTL delays the time to reach the maximum of about 1 hour while an hour earlier by AC + VD. Both CTL and AC + VD overestimate sensible heat flux in urban area, but AC + VD improve the simulation results from 1500 to 2000 LST especially in the dry days. Compared to dry day result, improvement effect for sensible heat flux by ECs is not obvious in wet day. Different from the dry day, the sensible heat flux is rapidly decreasing during the 1100–1800 LST in model results because rainfall often occurs in that duration. And simulated sensible heat flux is more sensitive to precipitation than observed.

Observed latent heat flux in dry days has the same features as the sensible heat flux in daytime (**Figure 3c**). The maximum of observed latent heat flux is about 200 W·m$^{-2}$, while the latent heat flux is seriously underestimated by CTL in urban area which further leads to error in humidity and temperature. But AC + VD result indicates that model performance for latent heat flux is much improved in both dry day and wet day (**Figure 3c** and **d**). The simulated diurnal pattern of latent heat flux by AC + VD is very close to the observation in the dry days although the value is still less than observation and there is phase deviation. There are still errors of latent heat flux simulated by AC + VD in the wet days.

Bowen ratio is a very important index for the energy balance. Because the latent heat flux is seriously underestimated by CTL, there are big simulation errors for Bowen ratio especially in nighttime, both in dry days and wet days (**Figure 4**). That problem has been largely solved by AC + VD even though there are still underestimated Bowen ratios especially from 600 to 1600 LST.

The heat flux change by AC + VD will further influence temperature and humidity in urban area. So next part we will force on evaluating the model performance of temperature and humidity at 2 m. For the dry day, temperature is obviously overestimated by CTL during the
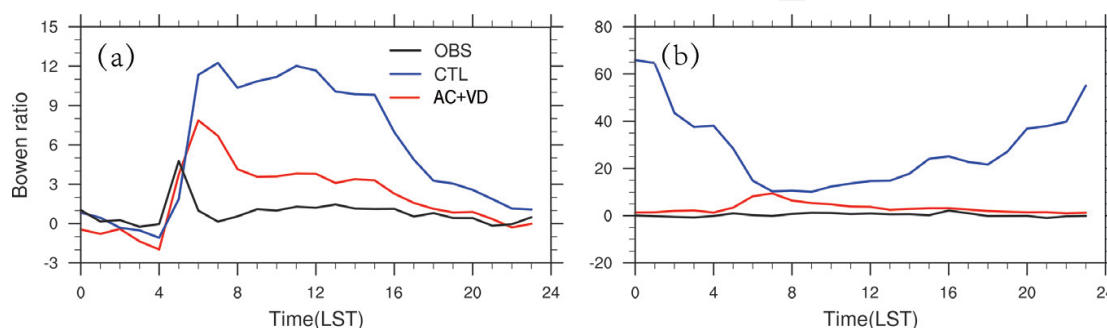


**Figure 4.** Averaged diurnal pattern of Bowen ratio. (a) Dry day and (b) wet day.
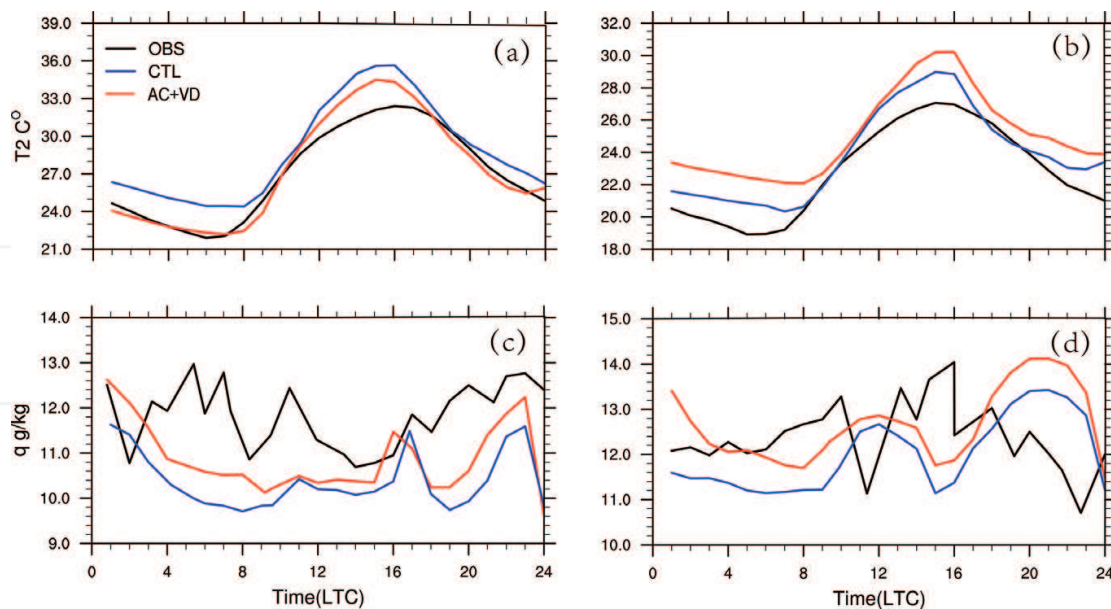
**Figure 5.** Averaged diurnal pattern of temperature (°C) and absolute humidity (g·kg$^{-1}$). (a) Temperature in dry day; (b) temperature in wet day; (c) absolute humidity in dry day; and (d) absolute in wet day.

whole day. But performance is largely improved by AC + VD especially in nighttime. Temperature at 2 m is decreased around 3° by AC + VD in nighttime which is very close to the observation (**Figure 5a**). There are still obvious errors during 1200–1600 LST. For the dry days, improvement for nighttime is still significant (2°) but not as good as wet days when compared to the observation (**Figure 5b**). Although AC + VD improves the temperature about 1.5°, the maximum simulation deviation still occurred from 1200 to 1600 LST. That is related to overestimating the sensible heat flux. Another error of phase is still in the simulation in dry day.

For the dry day, absolute humidity is underestimated by CTL during the whole day, while it is improved by AC + VD especially in nighttime (**Figure 5c**). For the wet day, absolute humidity is increasing from 1200 to 1600 because rainfall will more likely occur in this period. While simulated absolute humidity in both CTL and AC + VD lags behind the observation, increasing period is from 1800 to 2300 LST (**Figure 5d**). Simulated value is improved by AC + VD although the phase difference still remained in both dry day and wet day.

### 3.2. Effect on spatial distribution

294 meteorological stations are used to evaluate model performance of temperature and humidity spatial distribution. Spatial distribution of averaged temperature error shows that CTL overestimate daily mean temperature in most of urban station (**Figure 6a**), and the errors of most stations reach 1–2°. Errors of temperature are obviously reduced by EC in urban area and errors of about half stations <0.5° (**Figure 6b**). Both CTL and AC + VD underestimate daily mean absolute humidity at most urban stations. And there is no significant difference or improved effect by AC + VD in mean absolute humidity in urban area.
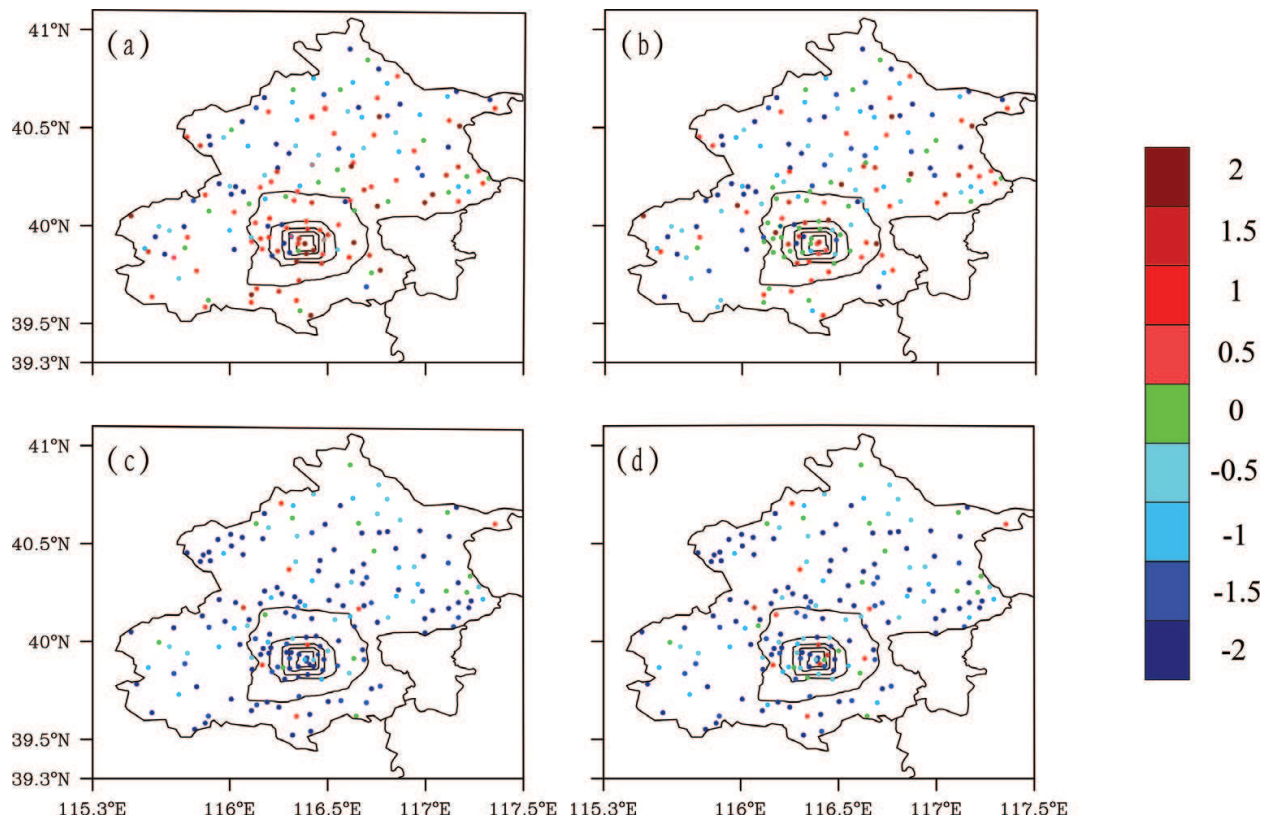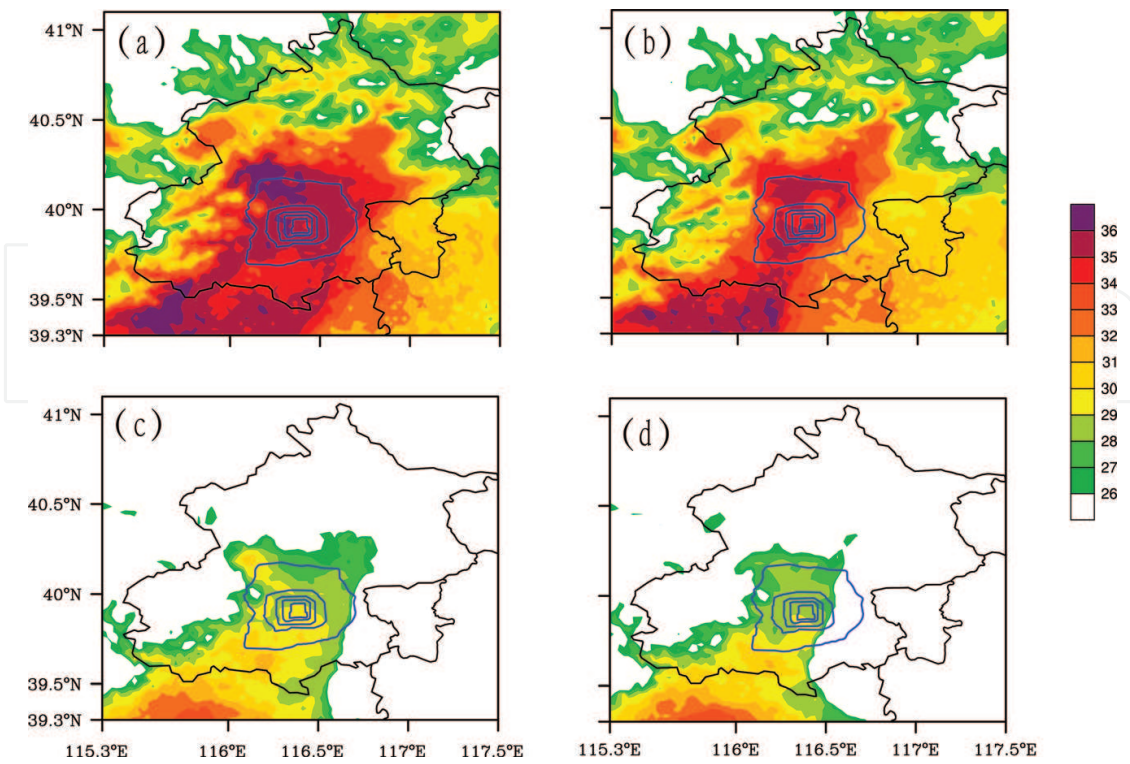
**Figure 6.** Spatial distribution of averaged temperature (°C) and absolute humidity (g·kg$^{-1}$) errors (difference between modeling and observation) at 2 m, the black circles show the second to sixth ring roads. (a) Temperature error in CTL; (b) temperature error in AC + VD; (c) absolute humidity error in CTL; and (d) absolute humidity error in AC + VD.

Maximum temperature (at 3 pm) simulated by CTL is more than 35°C in urban and suburban area in the dry day and 33°C in most of the plains (**Figure 7a**). While temperature is reduced to about 2° in AC + VD in both urban and suburban areas, and the area in which temperature is more than 36°C is obviously decreased (**Figure 7b**). There are the same characteristics for wet days (**Figure 7c** and **d**).
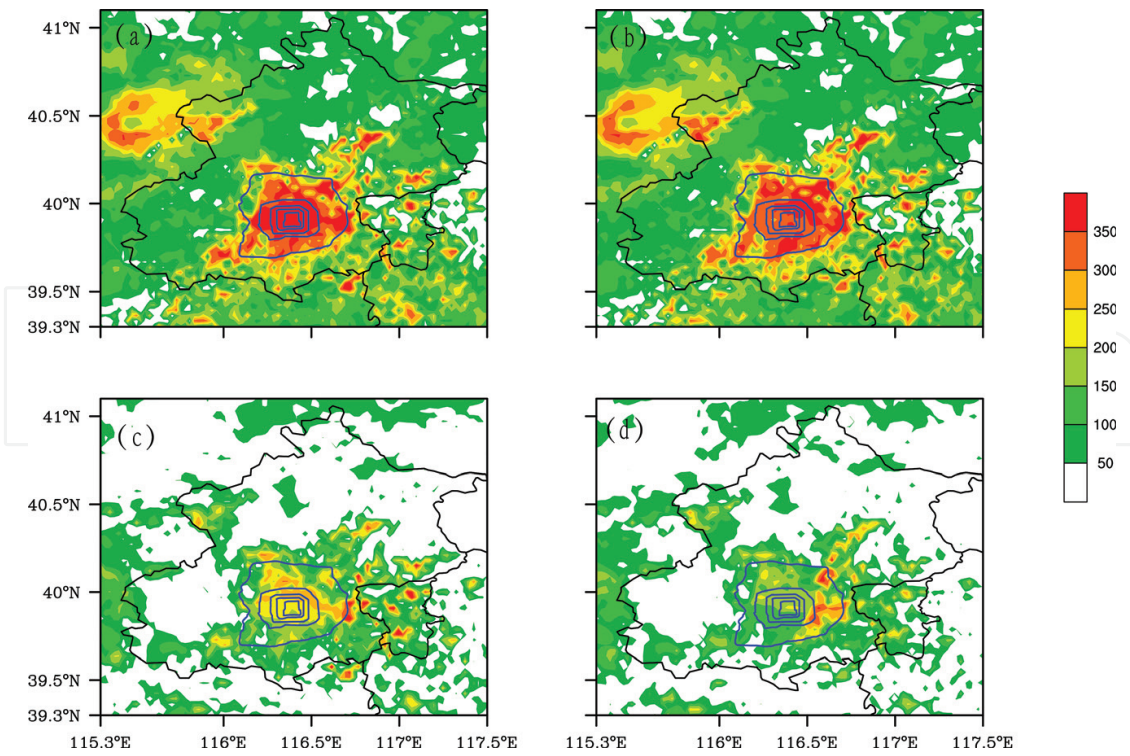
Spatial distribution of maximum sensible heat flux shows that sensible heat flux simulated by CTL in urban area is more than 350 W·m$^{-2}$ in the dry day (**Figure 8a**). The sensible heat flux simulated by AC + VD in most urban areas is about 320 W·m$^{-2}$ which is a little smaller than CTL (**Figure 8b**) in the dry day. And the maximum region (more than 350 W·m$^{-2}$) of sensible heat flux is also reduced by AC + VD. In the wet day, sensible heat flux maximum simulated by AC + VD is smaller about 50–100 W·m$^{-2}$ than CTL (**Figure 8c** and **d**).

Latent heat flux maximum simulated by CTL is less than 50 W·m$^{-2}$ in downtown area which is obviously underestimated compared to the observation in both dry day and wet day (**Figure 9a** and **c**). Simulation of latent heat flux in urban area by AC + VD improves the value to 100 W·m$^{-2}$ in dry day and 150 W·m$^{-2}$ in wet day (**Figure 9b** and **d**).

Maximum sensible heat flux released by air condition in CTL is more than 100 W·m$^{-2}$ in urban area, and there is a little difference between dry day and wet day. AC + VD reduce the maximum sensible heat flux released by the building's air condition in both dry days and wet

**Figure 7.** Spatial distribution of averaged temperature (°C) at 2 m in 3 pm. (a) Simulated by CTL in dry day; (b) simulated by AC + VD in dry day; (c) simulated by CTL in wet day; and (d) simulated by AC + VD in wet day.
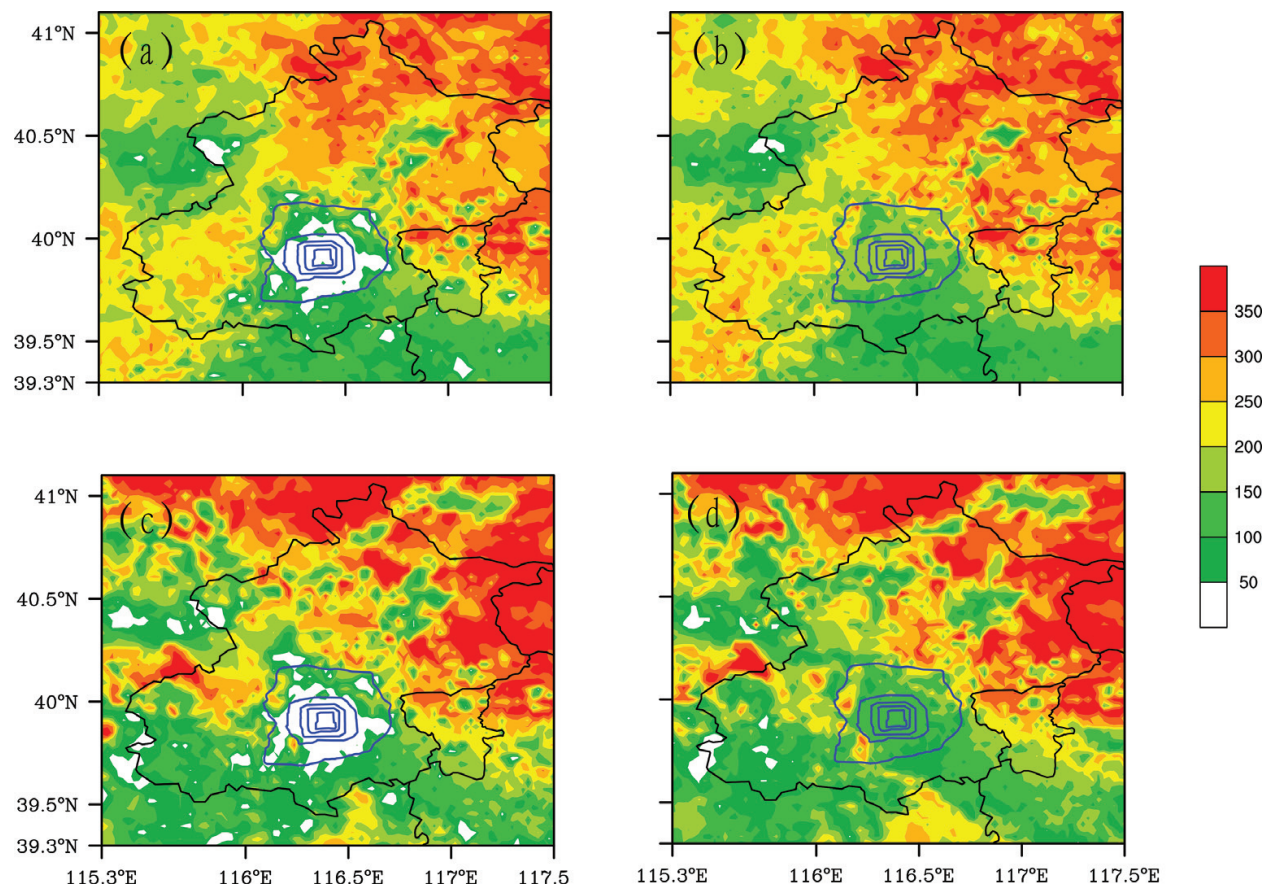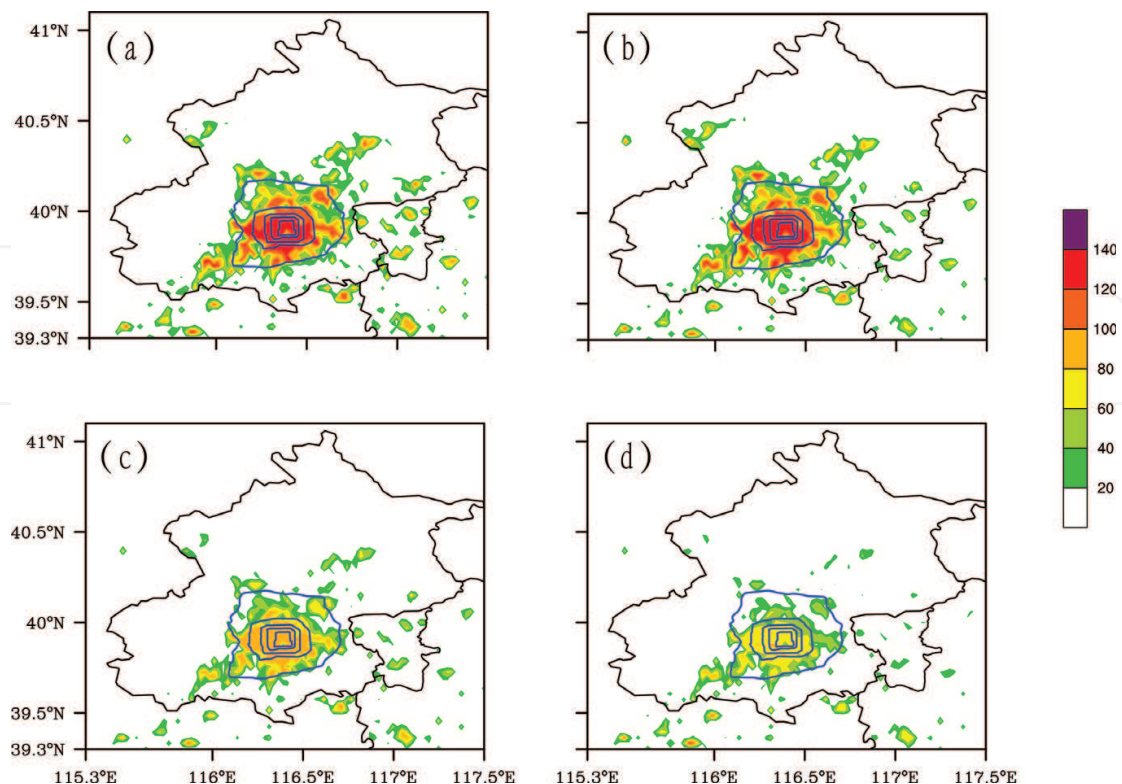


**Figure 8.** Spatial distribution of averaged sensible heat flux (W·m$^{-2}$) in 3 pm. (a) Simulated by CTL in dry day; (b) simulated by AC + VD in dry day; (c) simulated by CTL in wet day; and (d) simulated by AC + VD in wet day.

**Figure 9.** As in **Figure 8** but for latent heat flux.

days (**Figure 10a** and **c**). And sensible heat flux in dry day is obviously larger than wet days simulated by AC + VD (**Figure 10b** and **d**). That means sensible heat flux released by air condition in AC + VD is affected by outdoor temperature. Model performance of indoor and outdoor exchange is significantly improved by AC + VD.
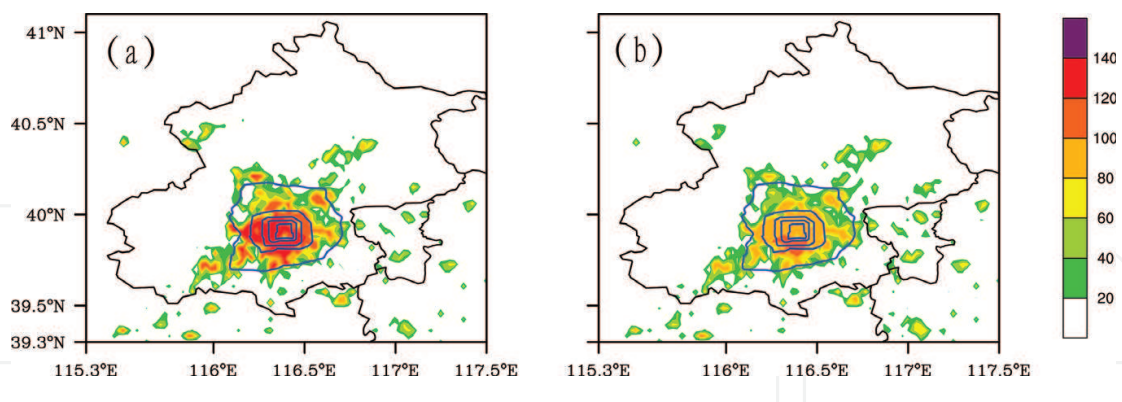
There is no latent heat flux released by air conditioning used in the potential temperature equation when coupled to the WRF/BEP + BEM in CTL. However, in AC + VD the maximum latent heat flux released is more than 120 $W \cdot m^{-2}$ in dry days and 80–100 $W \cdot m^{-2}$ in wet days (**Figure 11a** and **b**) over urban core areas.

### 3.3. Effect on wind field

The observed daytime change of urban area averaged wind speed appeared as single peak. The wind speed reaches maximum and minimum at 700 LST and 000 LST in summer in Beijing (**Figure 12a**). The diurnal feature of wind speed is well captured by CTL and AC + VD. However, CTL overestimated wind speed in daytime especially during 500–1000 LST. This problem has been largely solved by AC + VD (**Figure 12a**). RMSE is also obviously reduced by AC + VD in the whole day (**Figure 12b**).

**Figure 10.** Spatial distribution of sensible heat flux (W·m$^{-2}$) released by building air condition in 3 pm. (a) Simulated by CTL in dry day; (b) simulated by AC + VD in dry day; (c) simulated by CTL in wet day; and (d) simulated by AC + VD in wet day.



**Figure 11.** Spatial distribution of latent heat flux (W·m$^{-2}$) released by building air condition at 3 pm. (a) Simulated by AC + VD in dry day and (b) simulated by AC + VD in wet day.

Spatial distributions of wind speed by CTL show that the average wind speed in urban area is 3.5 W·m$^{-2}$ (**Figure 13a**), while the wind speed is reduced in AC + VD about 1.5 W·m$^{-2}$ (**Figure 13b**). The averaged wind speed simulated by AC + VD is about 1.8 W·m$^{-2}$. Wind speed in CTL is overestimated in all Beijing areas (**Figure 14a**). Spatial distributions of wind speed errors also indicated that wind speed error is obviously revised by AC + VD (**Figure 14b**).
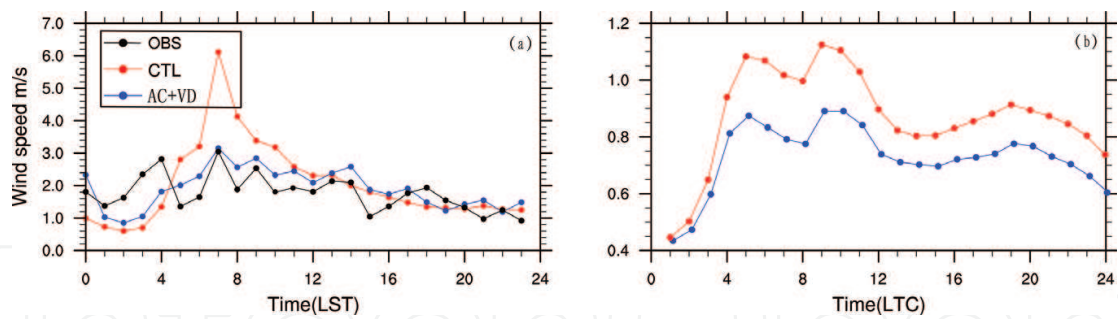
**Figure 12.** Averaged diurnal pattern of wind speed and its RMSE (W·m$^{-2}$). (a) Averaged of study period and (b) RMSE.
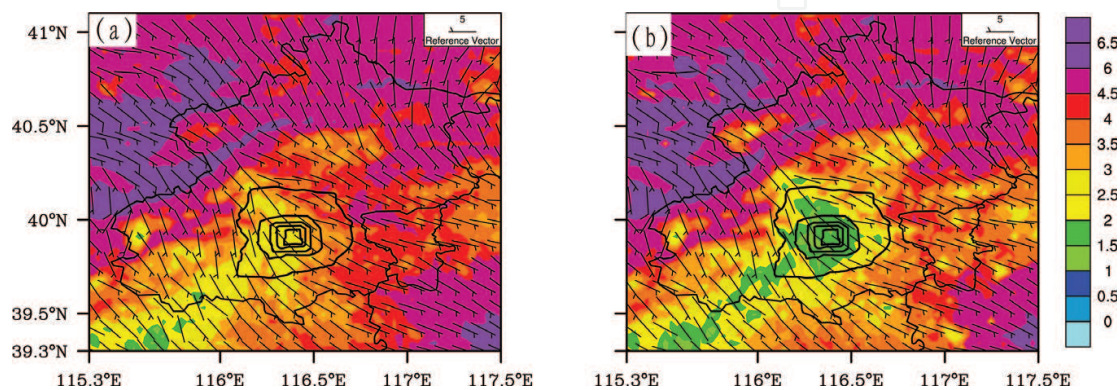


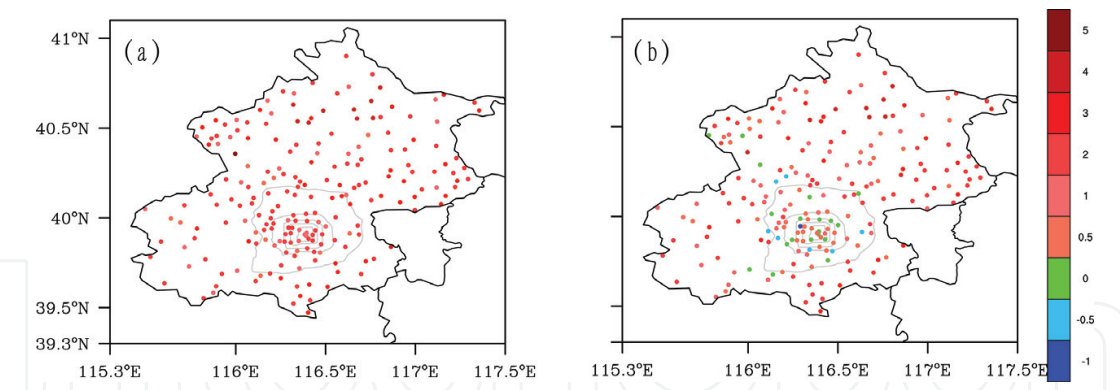**Figure 13.** Spatial distributions of wind speed and wind fields (W·m$^{-2}$). (a) CTL and (b) AC + VD.



**Figure 14.** Spatial distributions of wind speed errors (m·s$^{-1}$) (difference between modeling and observation) at 10 m. (a) CTL and (b) AC + VD.

## 4. Conclusions and discussions

A cooling tower scheme considering quantitative sensible and latent heat flux released from air condition was coupled to RMAPS. A mechanical drag coefficient formulation was implemented into the RMAPS to improve the representation of the wind speed in complex urban environments. The computing method is based on the heat transfer between temperature and humidity

and between condenser and outdoor inlet air. Two simulations use default RMAPS and improved RMAPS to estimate the improvement effect focusing on dry day and wet day, respectively. The cooling tower system in commercial area not only induces the significant increase of the anthropogenic heat partition by 90% of the total heat flux releasing as latent but also further changes the surface heat flux feature. When cooling tower is introduced, averaged surface latent heat flux in urban area is increased to about 60 $W \cdot m^{-2}$ with the peak of 150 $W \cdot m^{-2}$ in dry day and 40 $W \cdot m^{-2}$ with the peak of 150 $W \cdot m^{-2}$ in wet day. Further new cooling tower scheme improves the model performance of temperature and humidity. Maximum and minimum temperature error improves 2–3° especially in dry day. The drag coefficient formulation induced the simulated wind speed to about 2.5 $m \cdot s^{-1}$ that improve the wind speed error of about 2–3 $m \cdot s^{-1}$ in urban area.

## Acknowledgements

## Author details

Miao Yu[1,2]* and Shiguang Miao[1]

*Address all correspondence to: yumiao0926@126.com

1  Institute of Urban Meteorology, China Meteorological Administration, Beijing, China

2  State Key Laboratory of Severe Weather, Chinese Academy of Meteorological Sciences, Beijing, China

## References

[1] Population Reference Bureau. World Population Data Sheet. Population Reference Bureau; 2010

[2] Li Q, Li Q, Zhang H, Liu X, et al. Urban heat island effect on annual mean temperature during the last 50 years in China. Theoretical and Applied Climatology. 2004;**79**:165-174

[3] Li Y, Zhu L, Zhao X, Li S, Yan Y. Urbanization impact on temperature change in China with emphasis on land cover change and human activity. Journal of Climate. 2013;**26**:8765-8780

[4] Roth M. Review of urban climate research in (sub) tropical regions. International Journal of Climatology. 2007;**27**:1859-1873

[5] Hu Y, Dong W, He Y. Impact of land surface forcings on mean and extreme temperature in eastern China. Journal of Geophysical Research. 2010;**115**(D19)

[6] Kalnay E, Cai M. Impact of urbanization and land-use change on climate. Nature. 2003;**423**(6939):528-531

[7] Kalnay E, Cai M, Li H, Tobin J. Estimation of the impact of land-surface forcings on temperature trends in eastern United States. Journal of Geophysical Research. 2006;**111**(D6)

[8] Miao SG, Chen F, Lemone MA, et al. An observation al and modeling study of characteristics of urban heat island and boundary layer structures in Beijing. Journal of Applied Meteorology and Climatology. 2009;**48**(3):484-501

[9] Zhou LM, Dickinson RE, Tian YH, et al. Evidence for a significant urbanization effect on climate in China. Proceedings of the National Academy of Sciences of the United States of America. 2004;**101**:9540-9544

[10] Chen F, Kusaka H, Bornstein R, et al. The integrated WRF/urban modelling system: Development, evaluation, and applications to urban environmental problems. International Journal of Climatology. 2011;**31**(2):273-288

[11] Feng J, Wang Y, Ma Z, Liu Y. Simulating the regional impacts of urbanization and anthropogenic heat release on climate across China. Journal of Climate. 2012;**25**:7187-7203

[12] Allen L, Lindberg F, Grimmond CSB. Global to city scale urban anthropogenic heat flux: Model and variability. International Journal of Climatology. 2010;**31**:1990-2005

[13] Hinkel KM, Nelson FE. Anthropogenic heat island at Barrow, Alaska, during winter: 2001–2005. Journal of Geophysical Research. 2007;**112**:D06118

[14] Ichinose T, Shimodozono K, Hanaki K. Impact of anthropogenic heat on urban climate in Tokyo. Atmospheric Environment. 1999;**33**:3897-3909

[15] Zheng S, Liu S. Urbanization effect on climate in Beijing. Climate and Environmental Research. 2008;**13**(2):123-133

[16] Sailor D. A review of methods for estimating anthropogenic heat and moisture emissions in the urban environment. International Journal of Climatology. 2011;**31**:189-199

[17] Crutzen PJ. New directions: The growing urban heat and pollution "island" effect-Impact on chemistry and climate. Atmospheric Environment. 2004;**38**:3539-3540

[18] Flanner MG. Integrating anthropogenic heat flux with global climate models. Geophysical Research Letters. 2009;**36**:L02801

[19] Block A, Keuler K, Schaller E. Impacts of anthropogenic heat on regional climate patterns. Geophysical Research Letters. 2004;**31**:L12211

[20] Narumi D, Kondo A, Shimoda Y. Effects of anthropogenic heat release upon the urban climate in a Japanese megacity. Environmental Research. 2009;**109**:421-431

[21] Zhang G, Cai M, Hu A. Energy consumption and the unexplained winter warming over northern Asia and North America. Nature Climate Change. 2013;**3**:466-470

[22] He X, Jiang W, Chen Y, Liu G. Numerical simulation of the impacts of anthropogenic heat on the structure of the urban boundary layer. Chinese Journal of Geophysics. 2007;**50**(1): 75-83

[23] Ohashi Y, Genchi Y, Kondo H, Kikegawa Y, et al. Influence of air-conditioning waste heat on air temperature in Tokyo during summer: Numerical experiments using an urban canopy model coupled with a building energy model. Journal of Applied Meteorology and Climatology. 2007;**46**:66-81

[24] Munck C, Pigeon G, Masson V, Meunier F, et al. How much can air conditioning increase air temperatures for a City Like Paris, France? International Journal of Climatology. 2013; **33**(1):210-227

[25] Fan S. Assessment Report of Regional High Resolution Model (BJ-RUCv3.0). IUM Technical Note IUM/2015-1. Beijing, China: IUM; 2015

[26] Kusaka H, Kondo H, Kikegawa Y, Kimura F. A simple single-layer urban canopy model for atmospheric models: Comparison with multi-layer and slab models. Boundary-Layer Meteorology. 2001;**101**(3):329-358

[27] Salamanca F, Martilli A. A new building energy model coupled with an urban canopy parameterization for urban climate simulations–part II, Validation with one dimension off-line simulations. Theoretical and Applied Climatology. 2010;**99**:345-356

[28] Barlage M, Miao S, Chen F. Impact of physics parameterizations on high-resolution weather prediction over two Chinese megacities. Journal of Geophysical Research – Atmospheres. 2016;**121**:4487-4498

[29] Salamanca F, Martilli A, Tewari M, Chen F. A Study of the urban boundary layer using different urban parameterizations and high-resolution urban canopy parameters with WRF. Journal of Applied Meteorology and Climatology. 2011;**50**:1107-1128

[30] Gutiérrez E, Gonzalez J, Martilli A, Bornstein R, Arend M. Simulations of a heat wave event in New York City using a multilayer urban parameterization. Journal of Applied Meteorology and Climatology. 2015;**54**(2):283-301

[31] Adnot J. Energy Efficiency and Certification of Central Air Conditioners, Study for the D. G. Transportation-Energy (DGTREN) of the Commission of the EU. Ed. ARMINES. Final Report. Vol 1; April 2003. pp. 1-54

[32] Akbari H, Konopacki S. Energy savings of heat-island reduction strategies in Toronto, Canada. Energy. 2004;**29**:191-210

[33] Akbari H, Pomerantz M, Taha H. Cool surfaces and shade trees to reduce energy use and improve air quality in urban areas. Solar Energy. 2001;**70**(3):295-310

[34] Hassid S, Santamouris M, Papanikolaou N, Linardi A, Klitsikas N, Georgakis C, Assimakopoulos DN. The effect of the Athens heat island on air conditioning load. Energy and Buildings. 2000;**32**:131-141

[35] Kolokotroni M, Giannitsaris I, Watkins R. The effect of the London urban heat island on building summer cooling demand and night ventilation strategies. Solar Energy. 2006;**80**: 383-392

[36] Hsieh C-M, Aramaki T, Hanaki K. The feedback of heat rejection to air conditioning load during the nighttime in subtropical climate. Energy and Buildings. 2007;**39**:1175-1182

[37] Wen Y, Lian Z. Influence of air conditioners utilization on urban thermal environment. Applied Thermal Engineering. 2009;**29**:670-675

[38] Sailor DJ, Brooks A, Hart M, Heiple S. A bottom-up approach for estimating latent and sensible heat emissions from anthropogenic sources. In: Proceedings of the 7th Symposium on the Urban Environment. San Diego, CA: American Meteorological Society; 2007

[39] Zheng Y, Miao S, Zhang Q, et al. Improvements of building energy model and anthropogenic heat release from cooling system. Plateau Meteorology. 2015;**36**(2):562-574

[40] Martilli A, Clappier A, Rotach MW. An urban surface exchange parameterization for mesoscale models. Boundary-Layer Meteorology. 2002;**104**:261-304

[41] Zhang Y, Miao S, Dai Y, Bornstein R. Numerical simulation of urban land surface effects on summer convective rainfall under different UHI intensity in Beijing. Journal of Geophysical Research – Atmospheres. 2017;**122**(15):7851-7868

[42] Zhang Y, Miao S, Dai Y, Liu YH. Numerical simulation of characteristics of summer clear day boundary layer in Beijing and the impact of urban underlying surface on sea breeze [in Chinese]. Chinese Journal of Geophysics. 2013;**56**(8):2558-2573

[43] González JE, Bula-Silvera AJ. Conventional mechanical systems for efficient heating, ventilating, and air conditioning systems. In: Handbook of Integrated and Sustainable Buildings Equipment and Systems. Volume I: Energy Systems. New York: ASME Press; 2017

[44] Kusaka H, Kimura F. Coupling a single-layer urban canopy model with a simple atmospheric model: Impact on urban heat island simulation for an idealized case. Journal of the Meteorological Society of Japan. 2004;**82**:67-80

[45] Liang X, Miao S, Li J, et al. Surf: Understanding and predicting urban convection and haze. Bulletin of the American Meteorological Society. 2018;**99**(7):1391-1413

[46] Liao J, Tang L, Shao G, Qiu Q, Wang C, Zheng S, Su X. A neighbor decay cellular automata approach for simulating urban expansion based on particle swarm intelligence. International Journal of Geographical Information Science. 2014;**28**(4):720-738

[47] Olivo Y, Hamidi A, Ramamurthy P. Spatiotemporal variability in building energy use in New York City. Energy. 2017;**141**:1393-1401

[48] Yang B, Zhang Y, Qian Y. Simulation of urban climate with high-resolution WRF model: A case study in Nanjing, China, Asia-Pac. Journal of the Atmospheric Sciences. 2012;**48**(3): 227-241